Journal of Polymer Research (2022) 29:442
https://doi.org/10.1007/s10965-022-03279-w

ORIGINAL PAPER

Study of mechanical anisotropy of single walled carbon nanotube and polyvinyl alcohol polymer nanocomposite with a controlled alignment process

P. Kalakonda[1,2,3] · S. Banne[4] · P. B. Kalakonda[5]

Received: 24 June 2022 / Accepted: 13 September 2022

Abstract
Single Walled Carbon Nanotube (SWCNT) and polyvinyl alcohol (PVA) Polymer nanocomposites with the controlled mechanical alignment process have been used for structural anisotropy applications due to their desirable thermal and mechanical properties as well as their tunable degradability. In this work, we fabricated the nanocomposite scaffolds from forming hydrogels of individually dispersed SWCNTs and then partial backfilling with PVA polymer. Our fabrication method helps to minimize the aggregation of SWCNT and improve the degree of uniform dispersion of SWCNT in the polymer matrix. We further compared the mechanical properties in both directions of nanocomposite with different SWCNTs concentration. We observed that the tensile modulus increases more in the aligned direction than the normal to direction of SWCNTs at optimum 12wt% nanotube loading. Further, the nanotube networks suppress the polymer glass transition and extend the mechanical integrity of the polymer. The controlling internal orientation order of nanotubes with the help of alignment process in nanocomposite scaffolds can bring interesting highly structural anisotropic properties to a wide range of smart material industries such as aerospace, defense, and healthcare.

Keywords Polymer · SWCNT · Naanocomposites · Reinforcement · Anisotropy · Mechanical integrity

Introduction

The carbon nanotubes (CNTs) are the primary candidates for the mechanical reinforcement of all polymers for the next-generation multifunctional material architectures. These multifunctional nanocomposites can be obtained by integrating aligned CNTs with the polymer stretching, a larger CNTs aspect ratio, larger surface area per volume, homogeneous dispersion at high volume fraction, strong interfacial interactions with the polymers, and having exceptional thermal, electrical, optical and mechanical properties [1–8]. The CNTs are highly anisotropic, long-range orientational order resulting in a macroscopic anisotropy which is of great interest. For many smart material industrial applications, the main challenge lies in the alignment of CNTs and polymer stretching to take advantage of highly anisotropic characteristics.

The SWCNTs show limited reinforcement due to the many difficulties associated with the non-uniform dispersion, aggregation of nanotubes, slippage of CNTs to their smooth surfaces, and weaker interfacial interactions between polymer and nanotubes [6–10]. As a result of the direct dispersion of CNTs at higher loading into the polymer matrix, the widely used fabrication methods lead to the strengthening Young modulus well below the model-based estimations [1, 11]. When the high aspect ratio of SWCNTs (~ 1000) is well dispersed in a polymer matrix, they can significantly improve the mechanical properties. Recently, significant efforts have been attempted towards the improvement of

✉ P. Kalakonda
parvathalu.k@gmail.com

1 Department of Material Science and Engineering, Carnegie Mellon University, 5000 Forbes Avenue, Pittsburgh, PA 15213-3890, USA

2 Division of Physical Sciences and Engineering, King Abdullah University of Science and Technology (KAUST), Thuwal 23955-6900, Kingdom of Saudi Arabia

3 Department of Physics, Government City College (A), Osmania University, Hyderabad, India

4 Department of Chemistry, The Chines University of Hong Kong, Ma Liu Shui, Hong Kong

5 Department of Materials Science and Engineering, University of Wisconsin, Madison, USA

Published online: 29 September 2022

the effective degree of dispersion of CNTs in the polymer matrix [12, 13] and their interfacial interactions. As a result, many fabrication techniques have been developed based on the chemical/physical and mechanical fabrication methods [1, 14–21]. In fact, the researchers also developed many other methods such as mechanical force [22–27], magnetic [28–31], electric field [32–40], shear flows [18], and electrospinning [41, 42], to improve further the mechanical structures of polymer nanocomposites via alignment of nanotubes with the advantages of anisotropic properties of nanotubes.

For the higher degree of anisotropic composite scaffolds, the SWCNTs were aligned by uni-axially stretching of polymer nanocomposites at above polymer glass transition temperature [22]. The polymer nanocomposite melting process was undertaken by extruding [23, 24]. The alignment of the nanotube process was done by using melt-shear processing [25] where aligned polymer/nanotube nanocomposite fibers were fabricated along the direction of flow. Recently, a few methods were developed to fabricate conductive composite films by sliding a thin film of random polymer/nanotube ink solution between two glass substrates under pressure application [26]. Some other studies were also focused on making alignment of nanotubes in epoxy nanocomposites with the application of electric field by a layer-by-layer (LBL) method, where both the conductivity and modulus were improved in the direction of alignment [40]. Few other studies were also focused on making aligned nanotubes by using a flow process where the surfactant-containing nanotubes were slowly injected by a syringe needle into a polymer solution [14]. In fact, electro-spinning is also another technique that can be used to in-situ aligning CNTs in polymer nanofibers [41–50]. Recently, a few studies also focused on nanofiber arrays to fabricate highly anisotropic scalable nano-architecture [51–58]. However, these studies revealed a lower degree of anisotropy due to inter-spacing distance and porosity. It was observed that the degree of anisotropy is still well below the required value to use in many smart material industrial applications. As a result, the alignment of nanotubes and polymer stretching is far from a trial to scale up a degree of anisotropy for the smart material industry. Our fabrication method is a solution-based hydrogel/aerogel nanocomposite scaffolds to make an aligned nanocomposite which could help to scale up a degree of anisotropy for many industrial applications.

In this work, we have used our hypothesis of the controlled way of aligning polymer and SWCNTs with our solution-based fabrication method. Our fabrication method and controlled way alignment process of nanocomposites enable a higher degree of anisotropy by minimizing CNT interspace distance and increasing stronger interfacial interactions between CNTs and polymer. We have observed that there is an improvement in the tensile modulus of nanocomposite scaffolds which might be due to the stretching/alignment of nanotubes. The degree of anisotropy in tensile modulus improved desirably from 0.6 to ~ 1 (170%) in aligned nanocomposite scaffolds at 12 wt.% SWCNT loading compared to pristine PVA polymer. As a result, the alignment of nanotubes and polymer stretching in polymer nanocomposite scaffolds would lead to enhanced structural anisotropy of mechanical and electrical properties.

Methods and characterization

Materials Single-wall carbon nanotubes (SWCNTs)-CG-200 purchased from South West Nano Technologies, Pittsburgh, PA, USA. Polyvinyl alcohol (PVA) purchased from Bayer Pvt. Ltd, Pittsburgh, PA, USA.

Sample preparation

SWCNTs hydrogel/aerogel synthesis The SWCNTs (CG-200) dispersed in 1 wt % of the anionic *surfactant* sodium dodecyl-benzene-sulfonate (NaDDBS) with a 1:10 ratio and then followed by tip sonication (underwater bath) at 20% amplitude for two hours. To separate aggregation of SWCNTs, the dispersed (SWCNTs) solution was processed by centrifugation at 35,000 rpm for 19 min and then collected UV Vis spectrum to check CNT concentration. The CNT dispersed solution was placed at 60 °C under a vacuum oven until the formation of a gel. The SWCNTs were usually forming a gel at 0.3 wt% and then transfer a gel into various molds. These molds are placed in Petri dishes and sealed with dispensed parafilm to avoid shrinkage for about 12 h. The deionized (DI) water was filled slowly into a Petri dish and waited for about two hours. Then the water was replaced with 1.5 M HNO_3 acid to remove surfactant molecules and followed by rinsing with DI water until the neutral PH value. The SWCNT hydrogel floated in the water and then undergo for ethanol exchange to further CPD drying. Finally, we were able to make various shapes of SWCNT hydrogel/aerogels [57] (Fig. 1).

SWCNT/PVA nanocomposite sample preparation

The fabricated SWCNT hydrogels scaffolds possess enormous surface area per mass which is a crucial factor for efficient load transfer from polymers to SWCNT scaffold [57]. The pore diameters of SWCNTs scaffold are about 5–30 nm allowing easy infiltration of polymers. The PVA solution was prepared with different concentrations (0.1 to 1 wt %) to facilitate easy infiltration in the SWCNT scaffold. The SWCNTs hydrogel was transferred into 0.1 wt% PVA solution at 90 °C to infiltrate the polymer into the CNT network. We replaced polymer solution with each concentration at least for 3–4 h from 0.1 to 1 wt% until

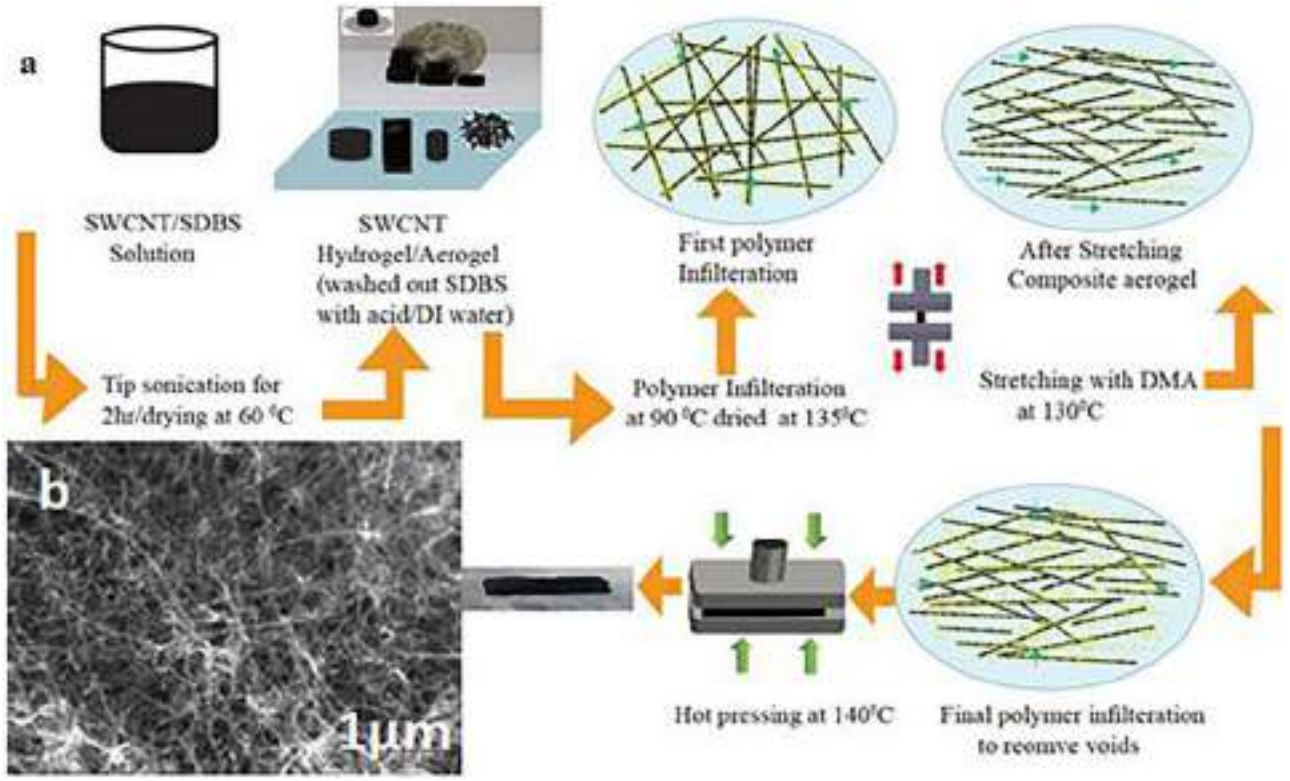

Fig.1 **a** Schematic illustrations of SWCNT/PVA aligned nanocomposites fabrication **b** SEM image of SWCNTs of aerogel

the required concentration of polymer in the scaffold. The polymer is in a rubbery state and has low viscosity at backfilling temperature of 90 °C, which facilitates easy infiltration of the polymer into the scaffold. The nanocomposite SWCNT/PVA scaffold was placed under vacuum at 60 °C to evaporate the solvent (water) out and dried completely the nanocomposite scaffold at 130 °C for a few hours. The nanocomposite scaffold sample was stretched 80–90% using the RSA-G2 DMA instrument (TA Instrument) in a controlled manner at 135 °C. And then the nanocomposite samples were placed in the polymer solution (0.2—0.5 wt %) to form an amorphous layer on the scaffold. Finally, the re-backfilled nanocomposite scaffold was dried at 140 °C for two hours and then followed by hot-pressed to remove voids in the nanocomposite sample.

Mechanical characterization

The tensile stress (σ) is characterized by a function of tensile strain (ϵ) at a strain rate of 1 mm/s with a 100 N load using an Instron Series IX version 8.31.00 series tabletop testing system (TA Instruments). For the tensile measurements, we used the standard sample to calibrate the device and then followed by the characterization samples.

Thermal analysis

Differential scanning calorimetric (DSC) measurements were carried out with a Q20 DSC (TA Instruments) at a heating rate of 3 °C/min. Thermo gravimetric analysis (TGA) was carried out under atmospheric air over a temperature range of 25 to 800 °C using a Q50 TGA (TA Instruments) at a heating rate of 3 °C/min.

Raman spectroscopy

The Raman spectra were collected with the help Raman confocal microscope (inverted) with a laser 785 nm and 20 × (0.40 NA) an objective lens. The lase power of 10mW, spot size of about 2 μm, and an exposure time of about 3-4 s were used for all samples to obtain high S/N spectra (Raman microscope, Reni Shaw- Leica Microsystems). Finally, the spectrum intensity was normalized by its G-band intensity.

Microstructure characterization

The porous 3-dimensional scaffold of carbon nanotube aerogel was imaged using scanning electron microscopy (FEI Quanta 600) to obtain high-resolution SEM images.

Electrical conductivity measurements

For electrical conductivity measurements of the nanocomposite scaffolds, we used copper foil leads to attach the short ends of the rectangular composite samples with silver paste, and resistance was measured using the two-probe contact method.

Results

In this study, we have used SWCNTs (average length ~ 1 µm, diameter ~ 1 nm) of solution-processed single-walled carbon nanotubes (SWCNTs) in the hydrogel, aerogel forms of 0.8 vol% as pre-formed scaffolds for fabrication of aligned nanocomposites. The SWCNTs were dispersed in a randomly oriented 3D network by Vander-Waals interaction within the scaffold (Fig. 1b). The scaffold possesses a pore diameter of 5-30 nm, a larger surface area per mass which is the essential factor for effective load transfer to the nanotubes and easy infiltration of the polymer into the SWCNT 3D network. The fabrication method of stretched/aligned nanocomposite scaffolds is described in the method section and the schematic is shown in Fig. 1a. The morphology of structural alignment of composites samples have observed with help of optical microscopy (S1).

Mechanical characterization was carried out for the aligned nanocomposite scaffold with various SWCNTs loading in both stretched orientation (parallel to CNTs) and normal to the stretching direction (normal to CNTs). The rectangular-shaped nanocomposite scaffold samples were used for all measurements with an average thickness of 150–200 µm. Figure 2a shows the tensile stress (σ) and tensile strain (ϵ) curve, for studying the mechanical characteristics of the scaffolds in both orientations. Figure 2b, c show the tensile stress vs tensile strain of pristine and nanocomposite scaffold at 12 wt% to see clear tensile modulus

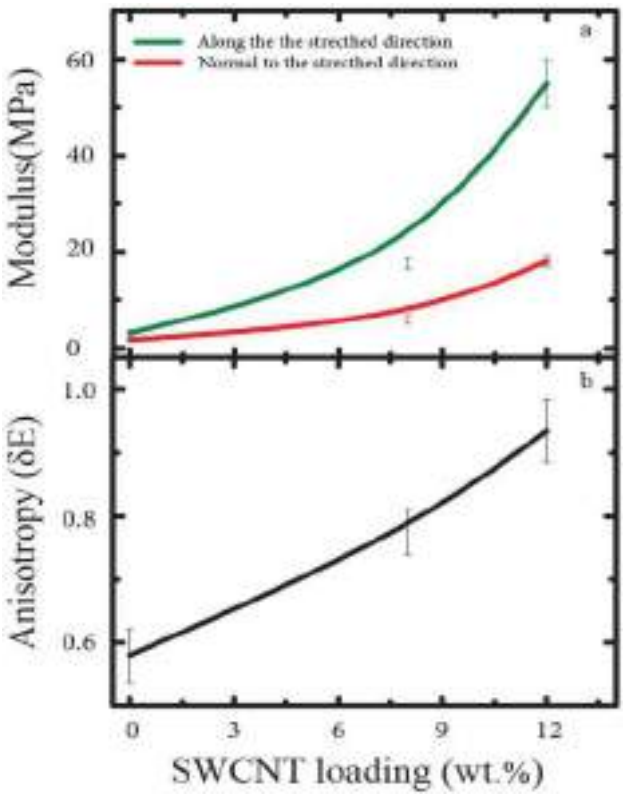

Fig. 3 **a** The modulus (E) of the nanocomposites along aligned direction (green) and transverse direction (red) with of nanotubes. **b** The degree of anisotropy in modulus of SWCNT/PVA nanocomposites as a function of SWCNT loading

measurements from the linear portion of the stress versus strain graph. We compared the mechanical properties of aligned nanocomposite in both directions with respect to the pristine PVA samples at room temperature.

The tensile modulus was calculated from the slope of the linear portion of the stress versus strain graph. The tensile modulus (*E*) of the pristine PVA polymer showed about 3.2

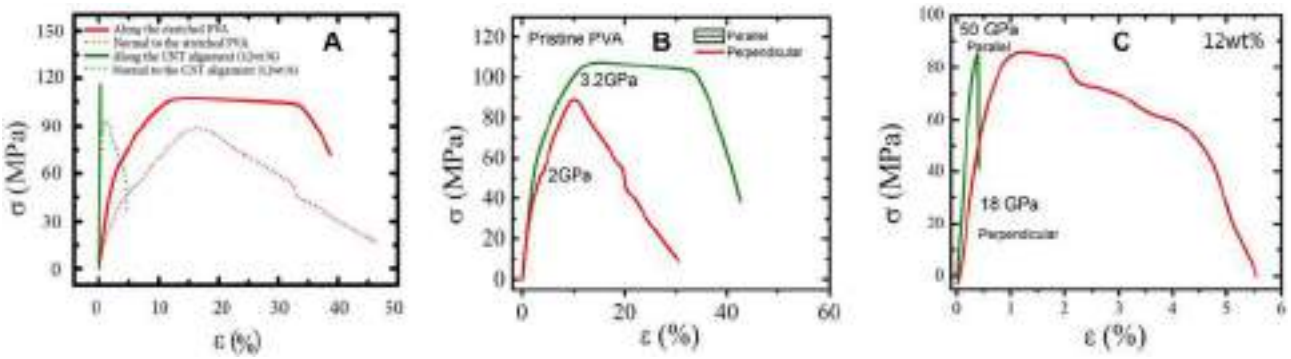

Fig.2 **A** The tensile stress (σ) versus tensile strain (ϵ) curves of pristine PVA and 12% SWCNT/PVA nanocomposites **B** The tensile stress (σ) versus tensile strain (ϵ) curves of pristine PVA **C** The tensile stress (σ) versus tensile strain (ϵ) curves of nanocomposites at 12 wt% (along stretching and normal to the stretching direction)

GPa along the stretched direction and 2 GPa along the normal to the stretching direction (Fig. 3a). The tensile modulus (*E)* of the composite scaffold increased dramatically along the stretched direction (55 GPa) compared to the perpendicular direction (18 GPa) at 12 wt% SWCNT loading (Fig. 3a). The tensile modulus increased 3times higher in the stretched direction than the normal to the CNT direction. However, the yield point was started for the nanocomposite scaffolds at a lower strain (> 1%) along the stretched direction compared to the perpendicular direction of CNTs. The ultimate tensile strength (UTS) of the nanocomposite scaffolds (at 12 wt.%) was higher by 1.3times higher in stretched direction with respect to the normal to the CNT direction.

The degree of anisotropy is defined as $\delta E = (E_L - E_T)/E_{Avg}$, modulus along aligned the direction (E_L), modulus along the transverse direction (E_T), and an average of the modulus (E_{Avg}). The degree of anisotropy in the tensile modulus of a pristine polymer and nanocomposite scaffolds in both orientations is shown in Fig. 3b. The tensile modulus of the nanocomposite scaffold (12 wt%) was increased about 27times along the stretched direction and 10times along the normal to the CNT orientation with respect to the pristine polymer. As a result, the degree of anisotropy in tensile modulus was increased desirably from 0.6 to ~ 1 in nanocomposite scaffolds compared to the pristine PVA polymer matrix.

Differential scanning calorimetry (DSC) analysis is used to examine the polymer crystallinity (Fig. 4). For a pristine polymer, the DSC curve on heating showed a sharp melting peak at 225 °C. This peak indicates stronger crystallinity since no peaks were observed on cooling. It is inferred that the sample does not have enough time to form crystals or to recrystallize. The endothermic peak temperature of the stretched nanocomposite scaffold was increased to about 5 °C and it was observed the glass transition peak was suppressed compared to the pristine polymer. A broader melting peak was observed for stretched nanocomposite scaffold compared to the pristine polymer which leads to the reduction of crystallinity.

The thermogravimetric analysis (TGA) is performed to elucidate the polymer stability (Fig. 5a). The mass loss in the polymer nanocomposite scaffold associated with burning off was reduced in the presence of the CNT network. The rate of mass loss showed that the degradation temperature of the composite scaffold was shifted to a higher temperature at 12 wt% SWCNT loading (Fig. 5b). The thermal stability was improved to 50 °C for the stretched nanocomposite scaffold compared to the pristine PVA polymer. The stretched nanocomposite scaffold sample weight was reduced by only 30% between 280 and 400 °C temperature and it was observed to remain stable until 280 °C. The aligned nanocomposite sample (12 wt%) showed 10% mass left even at 800 °C.

Raman spectroscopy is performed to verify the degree of SWCNT alignment in the polymer nanocomposite scaffold. The Raman spectra for a pristine polymer and aligned nanocomposite scaffold (12 wt%) are shown in Fig. 6. The characteristic peaks of nanotubes are higher than that arising from the pristine PVA. Though, we used the same power conditions, the peak intensity associated with pristine PVA is ultra-low (counts ~ 200) and can be considered

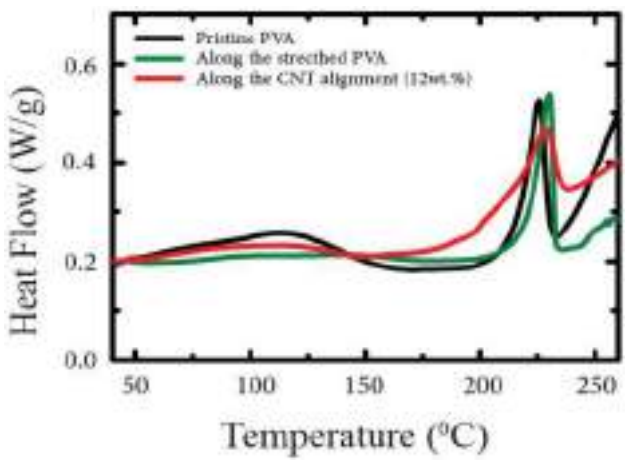

Fig. 4 Differential scanning calorimetry measurements of polymer and nanocomposites show a reduction in polymer crystallization in the composite with the orientation of nanotubes

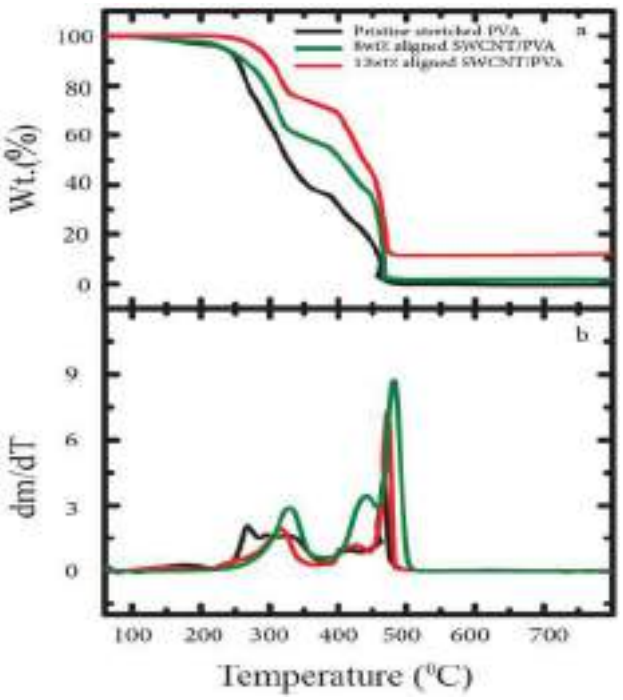

Fig. 5 **a** Thermogravimetric analysis (TGA) of stretched polymer and nanocomposite scaffold under atmospheric air **b** Examination of the rate of mass loss showed that degradation temperature shifted to higher temperature with orientation of nanotubes

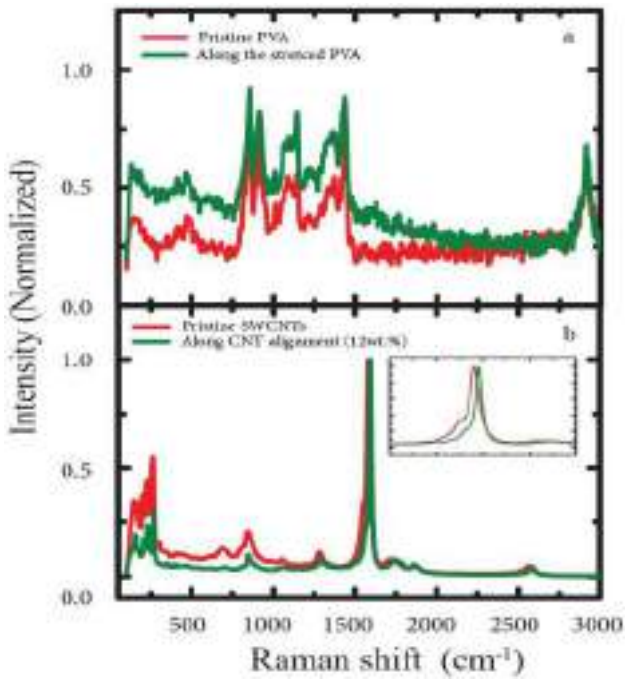

Fig. 6 Raman spectra of pristine polymer (**a**) and aligned SWCNT/PVA nanocomposites (**b**), showing different G- band peak shift for aligned polymer nanocomposite

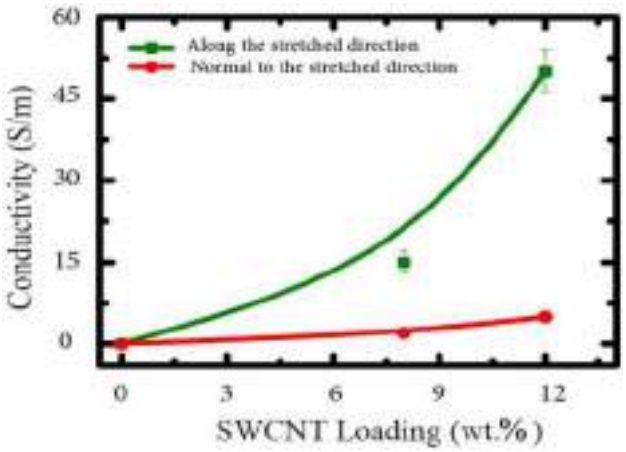

Fig. 7 Electrical conductivity of nanocomposites in aligned/transverse direction as a function of nanotube loading (solid lines are guide for eye)

negligible. As a result, the Raman spectrum of the aligned nanocomposite scaffold in Fig. 6 is similar to that of pristine nanotubes (four peaks). The peaks at around 150 cm^{-1}, are related to the Radial Breathing Modes (RBM), arising from the coherent vibration of carbon atoms in the radial direction. The RBM modes mainly depend on SWCNT diameter. The peak at about 1289 cm^{-1}, named D-band, arises in the presence of disorder from the defects located along the sidewalls of carbon nanotubes [58]. The peak at around 1582 cm^{-1}, called as G-band is attributed to the elongation of the carbon–carbon bonds along the longitudinal directional of the carbon nanotubes. The peak at about 2565 cm^{-1}, called G'-band is known as a second-order harmonic of the D-band [59]. All the characterization peaks associated with the stretched nanocomposite scaffolds have shifted 10 cm^{-1} to a higher wavenumber. The associated intensity of the aligned nanocomposite scaffold was observed to be greater than the randomly oriented composites.

The electrical conductivity of the stretched or aligned nanocomposite scaffolds was measured in both orientations via the two probe method (Fig. 7). In general, the electrical conductivity increases with increasing nanotube loading and it was found to be increased in stretched direction. The electrical conductivity of the nanocomposite scaffold at 12 wt% SWCNT loading in the stretched orientation was about 50 S/m and along the normal to the stretching direction was 5 S/m. The conductivity was found to be increased 10 times higher along the stretched direction as nanocompared to along the normal to the CNT direction.

Discussion

It is important to study the alignment/stretching effect of SWCNT/PVA nanocomposite scaffold to investigate anisotropy in mechanical properties. The stretching of a polymer and nanotubes was able to increase the stronger interfacial interactions between a polymer and nanotubes. As a result, the mechanical properties of aligned nanocomposite scaffolds were improved along with the stretched orientation compared to the normal to CNT orientation. The Raman spectra showed that the characterization peaks associated with the stretched nanocomposite scaffold shifted 10 cm^{-1} to a higher wavenumber. The DSC was also performed to elucidate the crystallinity of the nanocomposite scaffold, and the stretched nanocomposites reduced crystallinity, resulting in an extension of mechanical integrity. The stretched nanocomposite scaffolds were more thermally stable compared to the pristine polymer. The stretched polymer nanocomposite scaffolds have a wide range of applications in aerospace and other smart material industrial applications.

The stretching of a nanocomposite scaffold leads to stretching of the polymer as well as nanotubes which enhance the mechanical properties of nanocomposites due to an increase of stronger interfacial interactions between polymer chains and nanotubes. The stretching influenced stronger dependence on tensile modulus. The tensile modulus increased 17times along the stretching direction and 10 times along the normal to CNTs direction compared to the control pristine PVA polymer sample. The improvement

of the tensile modulus was clearly indicated due to the stretching/alignment of nanotubes. The degree of anisotropy in modulus increases as a function of SWCNT loading (Fig. 3b). As a result, the degree of anisotropy in tensile modulus improved desirably from 0.6 to ~ 1 in aligned nanocomposite scaffolds at 12 wt% SWCNT loading compared to pristine PVA polymer. We believe that this increase in anisotropy in mechanical properties due to the structural changes and a higher degree of alignment of polymer and nanotubes leads to stronger interfacial interactions.

As the SWCNTs concentration increases, the ultimate tensile strength (UTS) of nanocomposite scaffolds increases greatly compared to the pristine polymer. The stretching also slightly influenced tensile UTS. The UTS increased 1.5 times along the stretching direction and 1.1times along the normal to CNTs direction compared to the pristine PVA polymer samples. The UTS for nanocomposite scaffolds was observed to be lower in the normal to the CNT direction, and it would be due to "slippage" between nanotubes and the thermal motion of polymer chains. The stretchability decreased in stretched direction due to the brittleness of the materials (stronger interfacial interactions lead to larger tensile modulus).

The tensile modulus of stretched nanocomposite scaffolds leads to a drop with a further increasing SWCNT loading though the ideal/absolute value was still higher than the corresponding value for the nanocomposite scaffold without stretching application. The reinforcement efficiency would be lower at higher CNT loading for all polymer nanocomposites, and it would be attributed to the bundling of nanotubes, slippage between nanotubes, and non-uniform dispersion regardless of nanotube alignment. For better structural anisotropy, the 80–90% alignment of nanotubes and polymer stretching at 12 wt% SWCNT loading appears to be the optimum concentration. The CNT concentration (12 wt%) has a significant effect on enhancing polymer viscosity and nanotube packing. As a result, the lower free space and the higher resistance for CNTs to move and align in response to the stretching. The tensile modulus of nanocomposites in normal to the CNT direction was, in general, lower than that of the stretched direction, and it would be due to slippage, and weaker interfacial interactions between CNT-CNT, and CNT-polymer interactions. The polymer chain movements undergo lower restriction along the transverse direction rather than the aligned nanocomposites due to the presence of alternating polymer-rich regions (crystalline).

The Raman spectroscopy and DSC results are in good agreement with mechanical measurements. The Raman spectra suggest shifting 10 cm^{-1} of characterization peaks for stretched nanocomposite scaffolds. The associated intensity of stretched composite scaffolds observed was higher than the randomly oriented nanocomposites. As a result of Raman spectroscopy, the preferential orientation of alignment of SWCNTs due to the application of stretching is confirmed. The DSC results show that the endothermic peak height suppressed and shifted 5 °C towards higher temperatures for stretched nanocomposite scaffolds, and this may suggest reduced crystallinity due to the immobility of the polymer chains' motion, resulting in an extension of mechanical and structural integrity.

The thermal stability of stretched nanocomposite scaffolds increased above their decomposition temperature. The thermal stability improved to 50 °C for the stretched nanocomposite scaffold. The polymer near the CNTs might degrade slowly, which would shift the degradation temperature to higher temperatures (nanoconfinement effect). The improved thermal stability is due to efficient retardant additives of CNTs in polymer and leads to the presence of leftover mass even at 800 °C.

The electrical conductivity of the nanocomposite scaffold at 12 wt % SWCNT loading in the stretched orientation was about 50 S/m and 5 S/m along normal to the stretching direction. The increase in conductivity might be due to the reduction of contact resistance/ junction resistance and lower interfacial resistance between CNT-CNT, and CNT-polymer.

However, the observed enhancement of thermal, electrical, and mechanical properties of nanocomposite scaffold would be due to the stronger interfacial interaction between CNTs and polymer with the application of stretching. The stretching of the nanocomposite scaffold leads to the alignment of polymer and nanotubes which would improve the degree of anisotropy. The stretching helps to enhance mechanical properties in stretched direction, increase the brittleness of the scaffold, restrict polymer motion and improve the structural mechanical integrity between polymer and CNTs. The controlling of the internal orientational order of polymer and nanotubes in nanocomposite scaffolds can bring a tunable range of thermal, mechanical, and electrical properties, which would combine with anisotropic properties. These tunable nanocomposites might be useful for designing new applications in the smart nanomaterial industry.

Conclusion

We used solution-based hydrogel fabrication and a controlled mechanical alignment process renders them for structural anisotropy applications. We found that aligned SWCNT/PVA nanocomposite scaffolds possessed a desirable degree of anisotropy in mechanical properties. The controlled mechanical alignment process of nanocomposite reduces the mobility of the polymer, resulting in a suppression of polymer glass transition and an extension of mechanical structural integrity. The nanotubes and polymer are thermally stable above their degradation temperatures.

Our solution-based fabrication method along with a well-controlled internal orientation order of nanotubes in nanocomposite scaffolds can bring anisotropy in material properties, which would combine with the creation of highly structural anisotropic properties. These nanocomposites might be useful in designing new applications in the smart nanomaterial industry.

Supplementary Information The online version contains supplementary material available at https://doi.org/10.1007/s10965-022-03279-w.

Acknowledgements We thank to the Carnegie Mellon University, King Abdullah University of Science and Technology (KAUST) for financial support.

Declarations

Conflict of interest The authors declare that they have no competing financial interests or personal relationships that could have appeared to influence the work reported in this paper.

References

1. Coleman JN, Khan U, Blau WJ, Gun'ko YK (2006) Small but strong: a review of the mechanical properties of carbon nanotube-polymer composites. Carbon 44:1624–1652
2. Dresselhaus MS, Avouris P (2001) Introduction to carbon materials research. Top Appl Phys 80:1–9
3. Islam MF, Milkie DE, Kane CL, Yodh AG, Kikkawa JM (2004) Direct measurement of the polarized optical absorption cross section of single-wall carbon nanotubes. Phys Rev Lett 93:037404
4. Johnston DE, Islam MF, Yodh AG, Johnson AT (2005) Electronic devices based on purified carbon nanotubes grown by high-pressure decomposition of carbon monoxide. Nat Mater 4:589–592
5. Kalakonda P, Banne S (2017) Thermomechanical properties of PMMA and modified SWCNT composites. Nanotechnol Sci Appl 10:45–52
6. Kalakonda P, Cabrera Y, Judith R, Georgiev GY, Cebe P, Iannacchione GS (2015) Studies of electrical and thermal conductivities of sheared multi-walled carbon nanotube with isotactic polypropylene polymer composites. Nanomater Nanotechnol 5:2
7. Kalakonda P, Banne S, Kalakonda PB (2019) Enhanced mechanical properties of multiwalled carbon nanotubes/thermoplastic polyurethane nanocomposites. Nanomater Nanotechnol 9:1–7
8. Kalakonda P, Kalakonda PB, Banne S (2021) Studies of electrical, thermal, and mechanical properties of single-walled carbon nanotube and polyaniline of nanoporous nanocomposites. Nanomater Nanotechnol 11:1–8
9. Xie XL, Mai YW, Zhou XP (2005) Dispersion and alignment of carbon nanotubes in polymer matrix: a review. Mat Sci Eng R 49:89–112
10. Ma PC, Siddiqui NA, Marom G, Kim JK (2010) Dispersion and functionalization of carbon nanotubes for polymer-based nanocomposites: a review. Compos Part a-Appl S 41:1345–1367
11. Halpin JC, Kardos JL (1976) Halpin-Tsai Equations - Review. Polym Eng Sci 16:344–352
12. Ponnamma D, Sadasivuni KK, Grohens Y, Guo QP, Thomas S (2014) Carbon nanotube based elastomer composites - an approach towards multifunctional materials. J Mater Chem C 2:8446–8485
13. Zhang P, Zhou TF, He LC, Zhang SY, Sun J, Wang JJ, Qin CX, Dai LX (2015) Dispersion of multi-walled carbon nanotubes modified by rosemary acid into poly(vinyl alcohol) and preparation of their composite fibers. Rsc Adv 5:55492–55498
14. Vigolo B, Penicaud A, Coulon C, Sauder C, Pailler R, Journet C, Bernier P, Poulin P (2000) Macroscopic fibers and ribbons of oriented carbon nanotubes. Science 290:1331–1334
15. Gui XC et al (2011) A facile route to isotropic conductive nanocomposites by direct polymer infiltration of carbon nanotube sponges. ACS Nano 5:4276–4283
16. Kobashi K, Nishino H, Yamada T, Futaba DN, Yumura M, Hata K (2011) Epoxy composite sheets with a large interfacial area from a high surface area-supplying single-walled carbon nanotube scaffold filler. Carbon 49:5090–5098
17. Ci L, Suhr J, Pushparaj V, Zhang X, Ajayan PM (2008) Continuous carbon nanotube reinforced composites. Nano Lett 8:2762–2766
18. Ma WJ et al (2009) High-strength composite fibers: realizing true potential of carbon nanotubes in polymer matrix through continuous reticulate architecture and molecular level couplings. Nano Lett 9:2855–2861
19. Zeng Y, Ci L, Carey BJ, Vajtai R, Ajayan PM (2010) Design and reinforcement: vertically aligned carbon nanotube-based sandwich composites. ACS Nano 4:6798–6804
20. Zhang L, Xu W, Luo XG, Wang JN (2015) High performance carbon nanotube based composite film from layer-by-layer deposition. Carbon 90:215–221
21. Liu YD, Kumar S (2014) Polymer/carbon nanotube nano composite fibers-a review. Acs Appl Mater Inter 6:6069–6087
22. Jin L, Bower C, Zhou O (1998) Alignment of carbon nanotubes in a polymer matrix by mechanical stretching. Appl Phys Lett 73:1197–1199
23. Thostenson ET, Chou TW (2002) Aligned multi-walled carbon nanotube-reinforced composites: processing and mechanical characterization. J Phys D Appl Phys 35:L77–L80
24. Zhang Y, Iijima S (1999) Formation of single-wall carbon nanotubes by laser ablation of fullerenes at low temperature. Appl Phys Lett 75:3087–3089
25. Haggenmueller R, Gommans HH, Rinzler AG, Fischer JE, Winey KI (2000) Aligned single-wall carbon nanotubes in composites by melt processing methods. Chem Phys Lett 330:219–225
26. Najeeb CK, Chang J, Lee JH, Kim JH (2011) Fabrication of aligned ultra-thin transparent conductive films of single-walled carbon nanotubes by a compression/sliding method. Scripta Mater 64:126–129
27. Mecklenburg M, Mizushima D, Ohtake N, Bauhofer W, Fiedler B, Schulte K (2015) On the manufacturing and electrical and mechanical properties of ultra-high wt.% fraction aligned Mwcnt and randomly oriented cnt epoxy composites. Carbon 91:275–290
28. Smith BW, Benes Z, Luzzi DE, Fischer JE, Walters DA, Casavant MJ, Schmidt J, Smalley RE (2000) Structural anisotropy of magnetically aligned single wall carbon nanotube films. Appl Phys Lett 77:663–665
29. Casavant MJ, Walters DA, Schmidt JJ, Smalley RE (2003) Neat macroscopic membranes of aligned carbon nanotubes. J Appl Phys 93:2153–2156
30. Fischer JE, Zhou W, Vavro J, Llaguno MC, Guthy C, Haggenmueller R, Casavant MJ, Walters DE, Smalley RE (2003) Magnetically aligned single wall carbon nanotube films: preferred orientation and anisotropic transport properties. J Appl Phys 93:2157–2163
31. Choi ES, Brooks JS, Eaton DL, Al-Haik MS, Hussaini MY, Garmestani H, Li D, Dahmen K (2003) Enhancement of thermal and electrical properties of carbon nanotube polymer composites by magnetic field processing. J Appl Phys 94:6034–6039
32. Krupke R, Hennrich F, Kappes MM, Lohneysen HV (2004) Surface conductance induced dielectrophoresis of semiconducting single-walled carbon nanotubes. Nano Lett 4:1395–1399

33. Liu XM, Spencer JL, Kaiser AB, Arnold WM (2004) Electric-field oriented carbon nanotubes in different dielectric solvents. Curr Appl Phys 4:125–128
34. Chen CX, Zhang YF (2006) Manipulation of single-wall carbon nanotubes into dispersively aligned arrays between metal electrodes. J Phys D Appl Phys 39:172–176
35. Chen Z, Yang Y, Chen F, Qing Q, Wu Z, Liu Z (2005) Controllable interconnection of single-walled carbon nanotubes under Ac electric field. J Phys Chem B 109:11420–11423
36. Martin CA, Sandler JKW, Windle AH, Schwarz MK, Bauhofer W, Schulte K, Shaffer MSP (2005) Electric field-induced aligned multi-wall carbon nanotube networks in epoxy composites. Polymer 46:877–886
37. Kamat PV, Thomas KG, Barazzouk S, Girishkumar G, Vinodgopal K, Meisel D (2004) Self-assembled linear bundles of single wall carbon nanotubes and their alignment and deposition as a film in a Dc field. J Am Chem Soc 126:10757–10762
38. Zhang RP, Zhu YF, Ma C, Liang J (2009) Alignment of carbon nanotubes in poly(methyl methacrylate) composites induced by electric field. J Nanosci Nanotechno 9:2887–2893
39. Ma C, Zhang W, Zhu YF, Ji LJ, Zhang RP, Koratkar N, Liang J (2008) Alignment and dispersion of functionalized carbon nanotubes in polymer composites induced by an electric field. Carbon 46:706–710
40. Zhu YF, Ma C, Zhang W, Zhang RP, Koratkar N, Liang J (2009) Alignment of multiwalled carbon nanotubes in bulk epoxy composites via electric field. J Appl Phys 105
41. Ko F, Gogotsi Y, Ali A, Naguib N, Ye HH, Yang GL, Li C, Willis P (2003) Electrospinning of continuons carbon nanotube-filled nanofiber yarns. Adv Mater 15:1161
42. Sen R, Zhao B, Perea D, Itkis ME, Hu H, Love J, Bekyarova E, Haddon RC (2004) Preparation of single-walled carbon nanotube reinforced polystyrene and polyurethane nanofibers and membranes by electrospinning. Nano Lett 4:459–464
43. Kalakonda P, Georgiev G, Cabrera Y, Judith R, Iannacchione G, Cebe P (2014) Thermal and electrical transport properties of sheared and un-sheared thin-film polymer/CNTs nanocomposites. MRS Proc 1660:Mrsf13–1660-tt03–21
44. Kalakonda P, Daly M, Xu K, Cabrera Y, Judith R, Iannacchione G, Cebe P (2013) Structure-electrical transport property relationship of anisotropic iPP/CNT films. MRS Proc 1499:Mrsf12–1499-n05–83
45. Kalakonda P, Gombos E, Hoonjan G, Georgiev G, Iannacchione G, Cebe P (2012) Electrical conductivity of anisotropic iPP carbon nanotube thin films. MRS Proc 1410:Mrsf11–1410-dd05–06
46. Niu H, Guo H, Kang L et al (2022) Vertical alignment of anisotropic fillers assisted by expansion flow in polymer composites. Nano-Micro Lett 14:153
47. Yakovenko O, Matzui L, Danylova G et al (2017) Electrical properties of composite materials with electric field-assisted alignment of nanocarbon fillers. Nanoscale Res Lett 12:471
48. Wang Z, Cao Y, Pan D, Hu S (2020) Vertically aligned and interconnected graphite and graphene oxide networks leading to enhanced thermal conductivity of polymer composites. Polymers 12:1121
49. Lei C, Xie Z, Wu K, Fu Q (2021) Controlled vertically aligned structures in polymer composites: natural inspiration, structural processing, and functional application. Adv Mater 33:2103495
50. Sierra-Romero A, Chen B (2018) Strategies for the preparation of polymer composites with complex alignment of the dispersed phase. Nanocomposites 4(4):137–155
51. Lee J, Stein IY, Kessler SS, Wardle BL (2015) Aligned carbon nanotube film enables thermally induced state transformations in layered polymeric materials. Acs Appl Mater Inter 7:8900–8905
52. Lee J, Stein IY, Devoe ME, Lewis DJ, Lachman N, Kessler SS, Buschhorn ST, Wardle BL (2015) Impact of carbon nanotube length on electron transport in aligned carbon nanotube networks. Appl Phys Lett 106
53. Stein IY, Wardle BL (2014) Morphology and processing of aligned carbon nanotube carbon matrix nanocomposites. Carbon 68:807–813
54. Stein IY, Lachman N, Devoe ME, Wardle BL (2014) Exohedral physisorption of ambient moisture scales non-monotonically with fiber proximity in aligned carbon nanotube arrays. ACS Nano 8:4591–4599
55. Cebeci H, Stein IY, Wardle BL (2014) Effect of nanofiber proximity on the mechanical behavior of high volume fraction aligned carbon nanotube arrays. Appl Phys Lett 104
56. Handlin D, Stein IY, de Villoria RG, Cebeci H, Parsons, EM, Socrate S, Scotti S, Wardle BL (2013) Three-dimensional elastic constitutive relations of aligned carbon nanotube architectures. J Appl Phys 114
57. Bryning MB, Milkie DE, Islam MF, Hough LA, Kikkawa JM, Yodh AG (2007) Carbon nanotube aerogels. Adv Mater 19:661
58. Monti M, Puglia D, Natali M, Torre L, Kenny JM (2011) Effect of carbon nanofibers on the cure kinetics of unsaturated polyester resin: thermal and chemorheological modelling. Compos Sci Technol 71:1507–1516
59. Romyen N, Thongyai S, Praserthdam P (2012) Alignment of carbon nanotubes in polyimide under electric and magnetic fields. J Appl Polym Sci 123:3470–3475